A Nonlinear Fluctuation-Dissipation Test for Markovian Systems

Kirsten Engbring,[1,*] Dima Boriskovsky,[2,*] Yael Roichman,[2,3] and Benjamin Lindner[4,1]

[1]*Physics Department of Humboldt University Berlin, Newtonstraße 15, 12489 Berlin, Germany*
[2]*The Raymond and Beverley School of Physics and Astronomy, Tel Aviv University, Tel Aviv 6997801, Israel*
[3]*The Raymond and Beverley School of Chemistry, Tel Aviv University, Tel Aviv 6997801, Israel*
[4]*Bernstein Center for Computational Neuroscience Berlin, Philippstraße 13, Haus 2, 10115 Berlin, Germany*

(Received 21 September 2022; revised 7 April 2023; accepted 8 May 2023; published 12 June 2023)

Fluctuation-dissipation relations (FDRs) connect the internal spontaneous fluctuations of a system with its response to an external perturbation. In this work we propose a nonlinear generalized FDR (NL FDR) as a test for Markovianity of the considered nonequilibrium system; i.e., the violation of the NL FDR indicates a non-Markovian process. Previously suggested FDRs are based on linear response and require a significant number of measurements. However, the nonlinear relation holds for systems out of equilibrium and for strong perturbations. Therefore, its verification requires significantly less data than the standard linear relation. We test the NL FDR for two theoretical model systems: a particle in a tilted periodic potential and a harmonically bound particle, each driven either by white noise (leading to Markovian test cases, which should obey the NL FDR) or by colored noise (resulting in non-Markovian systems, which may not obey the relation). The degree of violation is systematically explored for the non-Markovian variants of our theoretical models. For the particle in the harmonically bound potential, all statistical measures entering the NL FDR can be calculated explicitly and can be used to elucidate why the relation is violated in the non-Markovian case. In addition, we apply our formalism and test for Markovianity in an inherently out-of-equilibrium experimental system, a tracer particle, embedded in an active bath of self-propelled agents (bristlebots) and subject to a force applied by an external air stream. An experimental violation of the NL FDR is witnessed by introducing an additional timescale to the process, when using bristlebots with two metastable speed states.

DOI: 10.1103/PhysRevX.13.021034

Subject Areas: Interdisciplinary Physics, Soft Matter, Statistical Physics

I. INTRODUCTION

Markovian systems, in which the statistics of future states depends only on the present state of the system but not on its past, are an important class of stochastic models that can describe systems both in or far beyond thermodynamic equilibrium [1–3]. For Markov processes there exists an established mathematical framework in the form of the well-studied Fokker-Planck or master equations, which we can apply once we know that we are dealing with this kind of system. Whether a certain set of time series adheres to the Markov property is thus a first crucial step in model building for nonequilibrium systems when basic equilibrium principles do not apply.

Trivially, it is not a problem to test for the Markov property if unlimited amounts of data are available; however, in typical situations, such as in living and active systems, the trial number is severely limited. Thus, probing a system for Markovianity (or the lack thereof) is a nontrivial but crucial problem for which different solutions have been suggested [4–9]. Most of the tests are limited in dimensionality (i.e., to a single time-dependent variable) or require detailed balance or conservative forces. Thus, alternative methods that apply to general Markov models of nonequilibrium systems (lacking detailed balance or being driven by nonconservative forces) are called for.

If both the spontaneous activity of a system as well as its response to a time-dependent perturbation are experimentally accessible, generalized fluctuation-dissipation relations (FDRs) [10–14] can be applied to test for Markovianity [4,5]. By choosing an appropriate variable (the conjugated variable to the perturbation), the correlation

[*]These authors contributed equally to this work.

of the spontaneous fluctuations is proportional to the time-dependent mean value in response to switching off the static perturbation (perturbation arrest)—this is a necessary (but not sufficient) condition for the system being Markovian in the observed variables. Unfortunately, it turns out in specific applications, as for instance, the mechanosensory hair bundle of auditory hair cells [4], that the typical limited amount of experimental data obtained was insufficient for a proper distinction between Markovian and non-Markovian dynamics [5]. The noise level in such systems is too high in comparison to the signal of the linear response to a weak perturbation to be averaged out given the limited amount of data.

Here, we take a direct approach to overcome this challenge and enhance the detectability of a Markovianity violation relative to the noise level. We do so by going beyond the linear-response regime. Applying strong perturbations to the system enhances its response and relaxation back into its nonperturbed steady state. To analyze the response to strong perturbations, we develop a new *nonlinear* fluctuation dissipation relation (NL FDR, derived in Sec. II), which applies for Markovian systems that can be perturbed with a step stimulus of arbitrary strength. Such a stimulus paradigm is routinely used when cells are mechanically stretched by laser beams [15], the mechanosensitive hair bundle is deflected by a glas fiber [16], neurons *in vivo* are light activated by channel rhodopsin [17], or the intracellular calcium concentration responds to the sudden increase in concentration of a signaling molecule [18], to name but a few examples of nonequilibrium systems and perturbations.

We design a simple protocol (detailed in Sec. II) to determine the needed statistics for a multidimensional Markov process $\mathbf{x}(t)$. The protocol requires us to measure the stationary probability densities of $\mathbf{x}(t)$, $P_\varepsilon(\mathbf{x})$, and $P_0(\mathbf{x})$, in the presence and absence of a static perturbation ε, respectively. Using both probability densities, we define a new variable by the nonlinear transformation:

$$z(\mathbf{x}) = \left(\frac{P_\varepsilon(\mathbf{x})}{P_0(\mathbf{x})} - 1\right). \tag{1}$$

As we show in Sec. II, if the system is Markovian, in the new variable it has to obey the NL FDR,

$$C_{zz}(\tau) = \langle z(\tau)\rangle, \quad \tau > 0, \tag{2}$$

where $C_{zz}(\tau) = \langle z(\tau)z(0)\rangle_0$ is the autocorrelation of the conjugated variable in the unperturbed steady state and $\langle z(\tau)\rangle$ its response to the perturbation arrest. The relation is a necessary (but not sufficient) condition for $\mathbf{x}(t)$ to be a Markov process and, remarkably, it holds true for arbitrary perturbation amplitude. It looks similar to a previously derived relation [19] but differs by the definition of the conjugated variable.

We demonstrate the working of our nonlinear relation and the protocol for three different systems: (1) a particle diffusing over a tilted washboard potential (Sec. III), (2) a particle trapped in a harmonic potential (Sec. IV), and (3) an experimental system of a trapped styrofoam ball in an active bath of bristle robots (bristlebots); for the latter, see Fig. 1 and Sec. V. All systems are studied in a Markovian version [which should obey Eq. (2)] and a non-Markovian version (which potentially violates it).

Our test protocol for the general case is described in detail in Sec. II B. Briefly, we first measure the stationary probability densities $P_\epsilon(x)$ and $P_0(x)$ with and without the perturbation, respectively [Figs. 1(b) and 1(c)] and calculate from them $z(x)$ using Eq. (1) [solid green line in Fig. 1(c)]. Next, we obtain the system's response to the perturbation's arrest by averaging over many realizations of the process $\langle z(\tau)\rangle$. We obtain the response in terms of the conjugated variable by mapping $x(t)$ to $z(x(t))$ using the

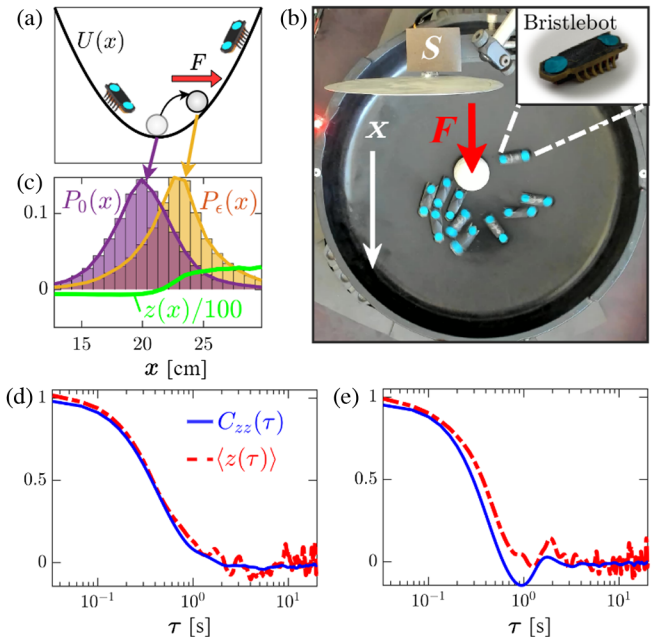

FIG. 1. The NL FDR test on an experimental setup far from equilibrium. An illustration of the system, bristle robots drive a styrofoam ball stochastically (a). Under constant force perturbation the average position of the ball shifts upward. Top view of the experimental system (b). The experimental realization of the model where a styrofoam ball is trapped in a bowl. It moves stochastically due to collisions with bristle robots (inset). A constant force perturbation is applied by a fan (labeled as "S") blowing a stream of wind on it. The stationary probability densities are measured at both steady states, either with or without the perturbation (c). From both distributions we calculate the conjugated variable Eq. (1) $z(x)$ (green line). A plot of the correlation function $C_{zz}(\tau)$ and the mean response $\langle z(\tau)\rangle$ reveals that the NL FDR holds for a single-velocity active bath (d) but can be violated if bristlebots with two velocity states are used (e); for more details, see Sec. V.

previously obtained $z(x)$. We calculate $C_{zz}(\tau)$ in the unperturbed state using the same map. We compare the response of the system to the autocorrelation [Figs. 1(d) and 1(e)] for different kinds of active baths, one apparently consistent with a Markov process [Fig. 1(d)] and one not [Fig. 1(e)]; see detailed discussion in Sec. V.

Our main result is the validation of the novel NL FDR and the resulting substantial reduction in the number of trials required to test for Markovianity in all three systems as compared to the linear FDR. In addition, we show that there is an optimal value of perturbation that provides the most sensitive test for Markovianity. Intuitively, the conditions for the optimal force can be understood from Fig. 1(c). The conjugated variable used in our NL FDR is calculated from the ratio of the two position distributions $P_\epsilon(x)$ and $P_0(x)$ according to Eq. (1). The sensitivity of our test relies on the dynamic range of $z(x)$ and our ability to measure it correctly both in the unperturbed state and for the transient response of the system with limited number of trials. To this end, we would like to work in conditions in which the overlap between $P_\epsilon(x)$ and $P_0(x)$ is small enough to allow for a large range in $z(x)$, on one hand, but not so large that it will fall into the far tails of one of the probabilities in which statistics are more limited.

Intuition on the underlying physics responsible for the violation of the NL FDR for non-Markovian processes is gained in Sec. IV by considering the simplest possible model, a harmonically bound particle. For this system we can calculate analytically the full statistics appearing in the NL FDR, both in the Markovian version (when the particle is driven by white noise) and in the non-Markovian version (when the noise is colored). We find that the finite correlation time of the colored noise affects the correlation function $C_{zz}(\tau)$ (appearing on the lhs of Eq. (2) but not at all the mean value $z(\tau)$ [appearing on the rhs of Eq. (2)]. This explains why pronounced correlations in the underlying noise process lead to the inequality of left- and right-hand sides in Eq. (2).

The paper is structured as follows. In Sec. II we introduce the derivation of the NL FDR and a protocol to determine the statistics of interest, $C_{zz}(\tau)$ and $\langle z(\tau)\rangle$, in simulations or experiments. In Sec. III, we explore random motion in an inclined washboard potential as a nonlinear example of a stochastic dynamics that lacks (even in the Markovian version) detailed balance. Section IV explores the simpler case of a harmonically bound particle, in which all statistics can be calculated analytically. Finally, in Sec. V we present an experimental test of the NL FDR of a macroscopic system composed of self-propelled bristlebots (an active bath) and a tracer ball. In Sec. VI we summarize our findings and give an outlook on future extensions and applications.

II. NONLINEAR FLUCTUATION-DISSIPATION RELATION

In the following section we derive the NL FDR and design a protocol to measure all relevant statistics.

A. Derivation

We consider a Markovian system characterized by a one-dimensional variable $x(t)$ that has been subject to a static perturbation ε for a sufficiently long time to reach steady state. The perturbation is switched off at time $t = t_{\rm off}$ (cf. Fig. 2). The time-dependent response of the mean value of a certain function $f[x(t)]$ for a time $t > t_{\rm off}$ can be written as follows:

$$\langle f[x(t)]\rangle = \int dx_1 \int dx_2 f(x_2) P_0(x_2, t|x_1, t_{\rm off}) P_\varepsilon(x_1), \quad (3)$$

where $P_\varepsilon(x_1)$ is the steady-state probability density for a constant perturbation and $P_0(x_2, t|x_1, t_{\rm off})$ is the conditional probability density with the perturbation switched off [$\varepsilon(t) = 0$]. Here we imply that $x(t)$ is a Markov process by assuming that $P_0(x_2, t|x_1, t_{\rm off})$ is completely independent of what happened to the system before time $t = t_{\rm off}$ (indicated by the index "0").

We can rewrite the above expression as follows:

$$\begin{aligned}\langle f[x(t)]\rangle - \langle f[x(t)]\rangle_0 &= \int dx_1 \int dx_2 f(x_2)\left(\frac{P_\varepsilon(x_1)}{P_0(x_1)} - 1\right) \\ &\times P_0(x_2, t|x_1, t_{\rm off}) P_0(x_1), \end{aligned} \quad (4)$$

in which we can identify

$$z(x) = \left(\frac{P_\varepsilon(x)}{P_0(x)} - 1\right) \quad (5)$$

as a conjugated variable for the specific perturbation $\varepsilon(t)$ applied to the system. We use in the following both $z(x)$ (with an x argument) as the nonlinear function that describes the mapping from x to z and $z(t) = z[x(t)]$ (with a time argument) as the new time-dependent observable.

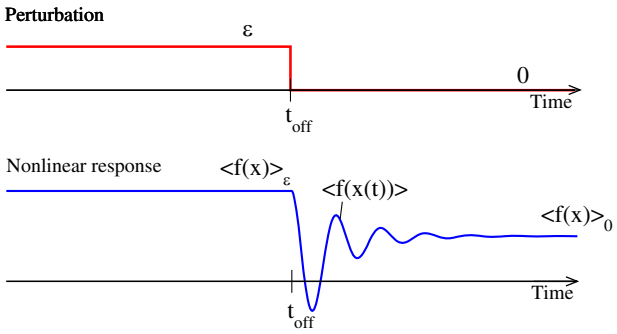

FIG. 2. Response to a steplike perturbation. A perturbation of strength ε (not necessarily small) is switched off at time $t_{\rm off}$ (top) and the time-dependent mean value of a nonlinear function $f[x(t)]$ (bottom) is observed.

For the conjugated variable $z(t)$, we find

$$\langle \delta f[x(t)] \rangle := \langle f[x(t]) \rangle - \langle f[x(t)] \rangle_0 = \langle f[x(t)] z(t_{\mathrm{off}}) \rangle_0 \quad (6)$$

for $t > t_{\mathrm{off}}$; i.e., the response of the system to the perturbation arrest is given by the stationary cross-correlation between the conjugated variable and the function $f[x(t)]$ in the absence of the perturbation (indicated by the index 0). The stationary mean of z without perturbation vanishes, irrespective of the perturbation amplitude ε,

$$\begin{aligned} \langle z \rangle_0 &= \int dx z(x) P_0(x) = \int dx \left(\frac{P_\varepsilon(x)}{P_0(x)} - 1 \right) P_0(x) \\ &= \int dx_1 P_\varepsilon(x_1) - \int dx_2 P_0(x_2) = 0, \end{aligned} \quad (7)$$

and also irrespective of whether the process is Markovian or not (we use only the steady state of the perturbed and unperturbed system).

Our relation Eq. (6) looks similar to Eq. (7) in Ref. [19] [Eq. (3.6) in the review Ref. [20]] but differs by the definition of the conjugated variable, which is in Refs. [19,20] solely based on the unperturbed density [$P_0(x)$ in our notation] while our variable $z(x)$ depends on both $P_0(x)$ and $P_\varepsilon(x)$.

If we choose the function f to be the conjugated variable itself, $f(x) = z(x)$, we obtain [taking into account that according to Eq. (7), $\langle \delta z(t) \rangle = \langle z(t) \rangle$, and measuring time since the switch-off by $\tau = t - t_{\mathrm{off}}$]:

$$\langle z(\tau) \rangle = \langle z(\tau) z(0) \rangle_0 = C_{zz}(\tau). \quad (8)$$

This is our key result, the NL FDR. It is trivially satisfied for $\tau \to \infty$ as response and correlations both go to zero in this limit (for Markovian and non-Markovian processes alike). It is also satisfied for both Markovian and non-Markovian processes at $\tau = 0$, which can be seen as follows. The left-hand side of Eq. (8) for $\tau = 0$ is given by the stationary average of $P_\varepsilon(x)/P_0(x) - 1$ over the density $P_\varepsilon(x)$:

$$\langle z(0) \rangle = \int dx \left(\frac{P_\varepsilon(x)}{P_0(x)} - 1 \right) P_\varepsilon(x) = \int dx \frac{P_\varepsilon^2(x)}{P_0(x)} - 1. \quad (9)$$

For the right-hand side of Eq. (8) we obtain at $\tau = 0$, the variance of $P_\varepsilon(x)/P_0(x) - 1$ in the unperturbed state:

$$\begin{aligned} \langle z(0) z(0) \rangle_0 &= \int dx \left(\frac{P_\varepsilon(x)}{P_0(x)} - 1 \right)^2 P_0(x) \\ &= \int dx \frac{P_\varepsilon^2(x)}{P_0(x)} - 1, \end{aligned} \quad (10)$$

i.e. the same as Eq. (9). Because we have not used the Markov property here, the NL FDR should be obeyed at $\tau = 0$ regardless of whether the process is Markovian or not; this does not hold true (as we demonstrate below) for nonvanishing lag times $\tau > 0$, for which Eq. (8) can be strongly violated for a non-Markovian $x(t)$.

We note that the entire line of argument can be repeated for an n-dimensional Markov process, $\mathbf{x} = (x_1, x_2, \ldots, x_n)$, where the conjugated variable is now defined using the multidimensional probabilities [this was introduced above in Eq. (1)]:

$$z(\mathbf{x}) = \left(\frac{P_\varepsilon(\mathbf{x})}{P_0(\mathbf{x})} - 1 \right). \quad (11)$$

In particular, the NL FDR attains the very same form as in Eq. (8). If we consider only a subset of variables $x_1(t), \ldots, x_k(t)$ of an n-dimensional Markov process (with $k < n$), this constitutes in general a non-Markovian projection of the process that does not have to obey Eq. (8).

Returning for the ease of notation to our one-dimensional example, if we assume a weak perturbation ($\varepsilon \ll 1$), Eq. (8) brings us with a few additional steps back to the known linear-response result [10–14]. This and related fluctuation-response relations have been tested for the sensory hair bundle [4] and also for colloidal particles driven by laser tweezers [13,21–23].

To compare to linear response, we insert

$$z(x) \approx \left. \frac{\partial \ln[P(x;\varepsilon)]}{\partial \varepsilon} \right|_{\varepsilon=0} \varepsilon = \varepsilon z_{LR}(x) \quad (12)$$

into Eq. (8) and obtain

$$\langle \delta z_{LR}(\tau) \rangle \approx \varepsilon \langle z_{LR}(\tau) z_{LR}(0) \rangle_0. \quad (13)$$

From the probability densities $P(x;\varepsilon) = P_\varepsilon(x)$ and $P(x;0) = P_0(x)$, we approximate $z_{LR}(x)$ by

$$z_{LR}(x) = \frac{\ln[P_\varepsilon(x)] - \ln[P_0(x)]}{\varepsilon} = \frac{1}{\varepsilon} \ln \left(\frac{P_\varepsilon(x)}{P_0(x)} \right) = \frac{\hat{z}(x)}{\varepsilon}. \quad (14)$$

In terms of the rescaled variable $\hat{z}$, the linear-response version of our theorem reads

$$\langle \delta \hat{z}(\tau) \rangle \approx \langle \hat{z}(\tau) \hat{z}(0) \rangle_0. \quad (15)$$

The approximate sign in this relation is solely due to

$$z(x) = \frac{P_\varepsilon(x)}{P_0(x)} - 1 \approx \ln \left(\frac{P_\varepsilon(x)}{P_0(x)} \right). \quad (16)$$

The approximate sign can be replaced with the equal sign only in the limit $\varepsilon \to 0$ when the density $P_\varepsilon(x)$ approaches $P_0(x)$ [by expanding the logarithm, $\ln\{[P_0 + (P_\varepsilon - P_0)]/P_0\} \approx 0 + (P_\varepsilon - P_0)/P_0 + \cdots$, we obtain with the first two terms the exact relation for the conjugated variable]. For all practical

purposes, a small value of ε may suffice for Eq. (15) being satisfied within the accuracy of measurement. A sufficiently small value will necessitate a large number of trials for two reasons. For one, the estimate of the conjugated variable in Eq. (14) will become more noisy with shrinking perturbation amplitude (unless compensated by an increase in trials), which results in increased unreliability in the estimates of the time-dependent mean value and of the correlation function in the unperturbed state. Secondly, the time-dependent mean value is also harder to distinguish against measurement noise if the difference in the two states (imposed by the weak perturbation) is only very small. Below we compare the left- and right-hand sides of Eq. (8) (the exact nonlinear relation) and of Eq. (15) (the approximate linear relationship) in order to illustrate the benefit of the nonlinear FDR.

Both of our theoretical example systems can be written as an overdamped noisy particle dynamics in a time-dependent potential $V(x,t;\varepsilon)$:

$$\dot{x} = -V'(x,t;\varepsilon) + s(t). \tag{17}$$

We look at two variants of Eq. (17). For the first we choose Gaussian white noise of intensity D, $s(t) = \sqrt{2D}\xi(t)$, where $\langle\xi(t)\rangle = 0$ and $\langle\xi(t)\xi(t')\rangle = \delta(t-t')$, resulting in $x(t)$ being a Markov process. For the second variant, $x(t)$ becomes a non-Markovian process by using $s(t) = \eta(t)$, where $\eta(t)$ is a temporally correlated (colored) Ornstein-Uhlenbeck process,

$$\tau_c\dot{\eta}(t) = -\eta(t) + \sqrt{2\sigma^2\tau_c}\xi(t), \tag{18}$$

in which $\xi(t)$ is again a white Gaussian noise. The low-pass filtered noise $\eta(t)$ is Gaussian and possesses an exponential correlation function, $\langle\eta(t)\eta(t')\rangle = \sigma^2\exp[-(|t-t'|/\tau_c)]$, with correlation time τ_c and variance σ^2. We note that the two-dimensional process $[x(t),\eta(t)]$ described by Eqs. (17) and (18) *is* Markovian whereas the one-dimensional projection $x(t)$ alone is not. By deliberately ignoring the second component of the two-dimensional process, we create a non-Markovian example process for which we can ask whether it obeys the NL FDR or not.

B. Protocol

Here we present the general protocol that is used to test the NL FDR on stochastic systems in the following sections. We illustrate it by means of the Brownian motion in a washboard potential in the Markovian version with white Gaussian noise [see Eq. (23) and surrounding discussion below]. As a specific perturbation of the dynamics, we consider a jumplike shift of the potential [see inset of Fig. 3(a) for the two potential shapes]. The perturbation, i.e., the shift of the force field by ε, is switched off exactly at the middle of the time window T, i.e., at time $t = T/2$:

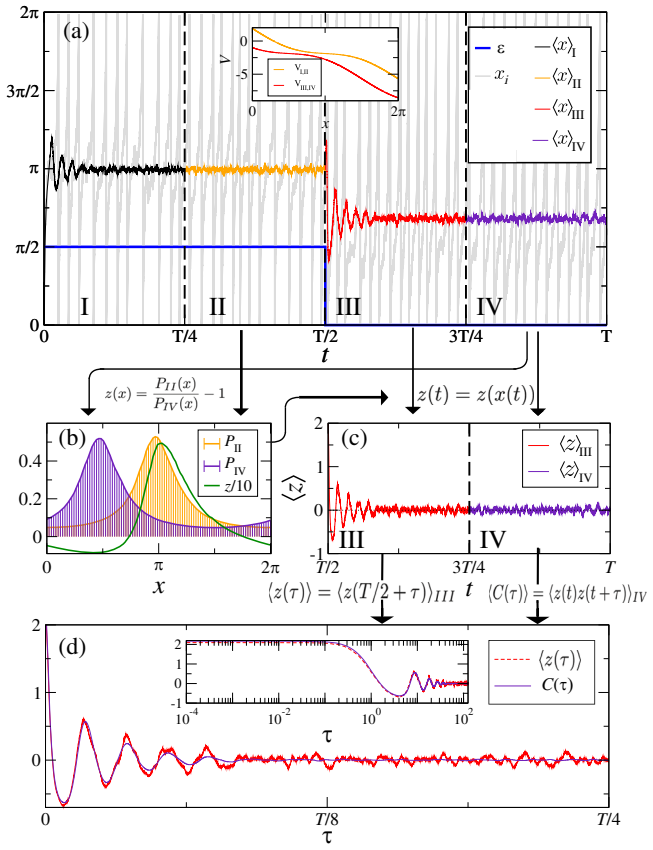

FIG. 3. Protocol to test the nonlinear fluctuation-dissipation relation for a small number of trials (here, $M = 1000$). Procedure is illustrated for a model of Brownian motion in an inclined periodic potential, Eq. (23) with white noise, solved with periodic boundary conditions for M subsequent trials; perturbation is a shift in the potential; see inset in (a). (a) Time window T is subdivided into four equal periods or phases; perturbation of size ε is applied in the first two phases of the time window and switched off at time $t = T/2$; we show a single trajectory x_i (gray line) and ensemble average $\langle x_i\rangle$ from the M trials (differently colored in the four phases). We obtain in phases I and III transient behavior in response to the sudden change in the external perturbation. In phases II and IV, when the system is approximately settled in the respective steady states, we estimate the stationary probability densities (b) by a combined time and ensemble average. By means of the two densities, the trajectories $x_i(t)$ can now be transformed to realizations of the conjugated variable $z_i(t)$ (c). Using the stored trajectories $x_i(t)$ from phases III and IV, we can estimate the ensemble mean of $z(t)$ in response to the perturbation arrest as well as the stationary correlation function $\langle z(t)z(t+\tau)\rangle_0$ in the absence of the perturbation. Comparison of the two functions confirms the NL FDR, Eq. (8) (d). Parameters are $F = 1.2$, $\varepsilon = \pi/2$, $D = 0.02$, time window $T = 10^3$, integration time step size $\Delta t = 10^{-2}$.

$$V(x,t;\varepsilon) = V[x - \varepsilon\Theta(T/2-t)]. \tag{19}$$

Here $\Theta(\tau)$ is the Heaviside function, which is zero and one for negative and positive arguments, respectively.

The following protocol is repeated for M subsequent trials; the simulation time window T of each trial has to be subdivided in four distinct periods of equal length $T/4$. In the first two periods, the perturbation is switched on, during the last two periods it is switched off. The protocol is as follows [cf. Fig. 3(a)].

(I) During the first period, the system reaches approximately the steady state corresponding to the perturbation being on.

(II) Via time and ensemble average, the steady-state density $P_\varepsilon(x) = P_{\mathrm{II}}(x)$ (for the constant perturbation ε) is measured and stored. We use the entire trajectory $x_i(t)$ within this period for all realizations $i = 1, \ldots, M$ to estimate a histogram for the probability to be at a certain $x \in [0, 2\pi]$.

(III) This period serves two purposes. For one, we measure M transient responses $x_i(T/2 + \tau)$ to the switch-off in the potential that happens at $t = T/2$ (at the beginning of this phase) and store them. Secondly, we let the system reach approximately the new (unperturbed) steady state.

(IV) The system is now in the new steady state and we can use the trajectories measured here to estimate the probability density $P_0(x) = P_{\mathrm{IV}}(x)$ in the absence of a perturbation. We store all the trajectories $x_i(t)$ for $i = 1, \ldots, M$.

The protocol requires a window T that is much longer than the relaxation times of the probability density (we cannot use an infinite T and that is why we use the word *approximately* in steps I and III). For this purpose, one may monitor time-dependent mean values [for our example system we choose $\langle x(t)\rangle$] and test whether they have reached approximately constant values in phases II and IV [cf. orange and purple lines in Fig. 3(a)].

With estimates of $P_\varepsilon(x)$ [steady-state distribution $P_{\mathrm{II}}(x)$ of phase II] and $P_0(x)$ [steady-state distribution $P_{\mathrm{IV}}(x)$ of phase IV] we can estimate the variable $z(x)$ via Eq. (5); both distributions and the new variable are shown in Fig. 3(b). We then use the responses $x_i(t)$ to the perturbation arrest from phase III to calculate the mean *transient* response of $z(\tau)$:

$$\langle z(\tau)\rangle \approx \frac{1}{M}\sum_{i=1}^{M} z[x_i(T/2+\tau)], \tag{20}$$

which is shown as a function of τ in Fig. 3(c).

We can now furthermore take the ensemble of trajectories $x_i(t)$ from phase IV and calculate the correlation function of $z(t)$ in the absence of a perturbation by a combined ensemble and time average:

$$C_{zz}(\tau) = \langle z(0)z(\tau)\rangle \approx \sum_{i=1}^{M}\int_{3T/4}^{T-\tau} dt \frac{z[x_i(t)]z[x_i(t+\tau)]}{M(T/4-\tau)}. \tag{21}$$

The correlation function can now be compared to the transient response [see Fig. 3(d)], resulting in a confirmation of the NL FDR Eq. (8) for a small M.

A quantitative measure to evaluate the degree of violation of Eq. (8) is the integrated relative squared deviation (RSD) Δ^2 between the two time-dependent functions (normalized by an integral over the transient itself):

$$\Delta^2 = \frac{\int_0^{T_c} d\tau[\langle z(\tau)\rangle - \langle z(t)z(t+\tau)\rangle]^2}{\int_0^{T_c} d\tau[\langle z(\tau)\rangle]^2}. \tag{22}$$

By looking at the noisy functions in Fig. 3(d), it becomes clear that we should not use an excessively long time T_c for this integral because at large lag times we will mainly collect measurement noise in both integrals in the numerator and the denominator. We have chosen the integration window T_c according to visual inspection to capture the main part of the correlation and the transient response. A reasonable rule of thumb seems to be to terminate the integration once $\langle z(\tau)\rangle$ has reached the standard deviation of the measurement noise.

III. RANDOM MOTION IN AN INCLINED PERIODIC POTENTIAL—A NONLINEAR NONEQUILIBRIUM EXAMPLE

We consider the above example in more detail for both white noise (the Markovian case, used already in Fig. 3) and colored noise (the non-Markovian case, in which the NL FDR does not have to be obeyed). For the convenience of the reader, we state the equation for the specific setup (with periodic boundary conditions in $x \in [0, 2\pi]$):

$$\dot{x} = F - \sin[x - \varepsilon\Theta(T/2 - t)] + s(t). \tag{23}$$

Without perturbation ($\varepsilon = 0$) and with $s(t) = \sqrt{2D}\xi(t)$, this equation describes a plethora of physical phenomena [1,24]. It is in both Markovian and non-Markovian versions a nonequilibrium system, because for nonvanishing bias $F \neq 0$ there is a steady probability current running through the system [1] and the steady-state probability density deviates from the Boltzmann distribution expected in thermodynamic equilibrium [25].

We test the NL FDR for both Markovian and non-Markovian cases: as in Fig. 3 we choose a strong perturbation of $\varepsilon = \pi/2$ but use a smaller bias force: it is now at its critical value, $F = 1$, which results in less pronounced oscillatory behavior than for the stronger bias used in Fig. 3.

For the Markovian case shown in Fig. 4 the stationary density distributions P_ε and P_0 are of the same form but shifted by the perturbation parameter ε (densities can also be analytically expressed by quadrature; see, e.g., Ref. [1]). To test the NL FDR, Eq. (8), we use in Fig. 4(b) a rather small ensemble size of $M = 100$, for which the agreement

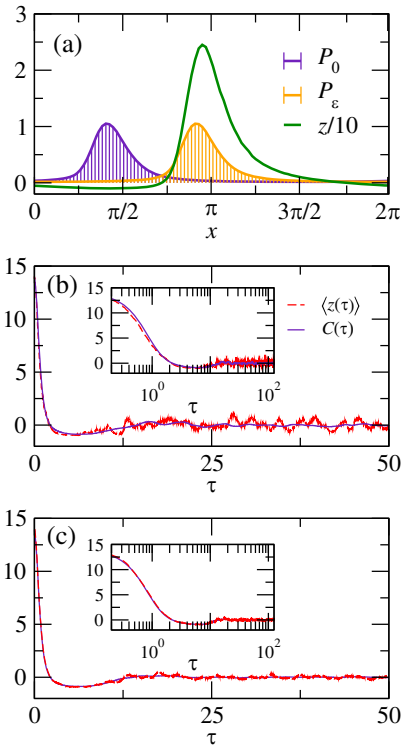

FIG. 4. Random motion in an inclined periodic potential—Markovian case [$s(t)$ white noise with $D = 0.02$]. Dynamics Eq. (23) with $F = 1$, $\varepsilon = \pi/2$, $T = 1000$, $\Delta t = 0.01$. Stationary probability densities in absence and presence of the perturbation and the conjugated variable $z(x)$ (a). Comparison of transient response and stationary correlation function for trial number $M = 100$ (b) and $M = 1000$ (c).

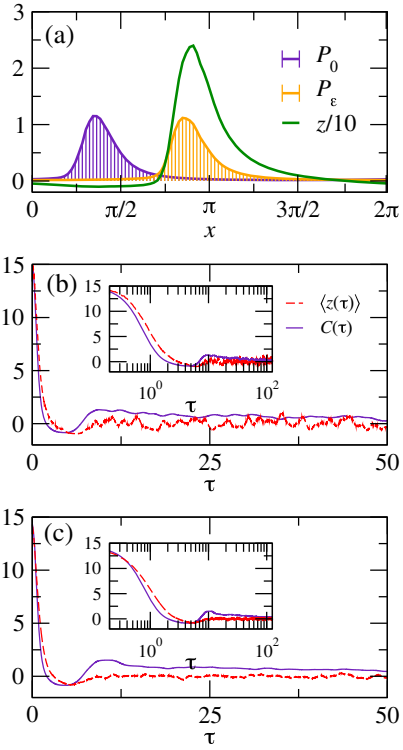

FIG. 5. Random motion in an inclined periodic potential—non-Markovian case. Equation (23) with $s(t)$ being colored Gaussian noise obtained from Eq. (18) with correlation time $\tau_c = 100$ and variance $\sigma^2 = 0.2$. Other parameters as in Fig. 4. Stationary densities and conjugated variable $z(x)$ (a). Comparison of transient response and stationary correlation function for $M = 100$ (b) and $M = 1000$ (c).

between the time-dependent mean value and the correlation function is already remarkably good. For a still reasonable ensemble size of $M = 1000$ [Fig. 4(c)] the agreement is overall quite excellent. To compare the two time-dependent functions in more detail, we show them with a logarithmic axis in the insets.

For the non-Markovian case, Fig. 5, the parameters of the colored noise σ^2 and τ_c were chosen such that the transient response of the system is similar in form and strength to that of the Markovian case in Fig. 4. We recall that in the non-Markovian case we cannot expect that the NL FDR is obeyed; indeed, a violation of Eq. (8) becomes already apparent for the small ensemble size of $M = 100$ [Fig. 5(b)] and even more clearly for $M = 1000$ [Fig. 5(c)]. The correlation function displays more pronounced oscillatory features (note the maximum around $\tau = 10$) and a stretched decay, most likely determined by the long correlation time of $\tau_c = 100$ of the intrinsic colored noise—the transient response of the mean value (red line) lacks this long transient.

For a quantitative analysis we inspect the RSD, Eq. (22), as a function of the perturbation amplitude ε [Fig. 6(a)] and trial number M [Fig. 6(b)]. For weak perturbation, estimates of the statistics are unreliable and the RSD for Markovian and non-Markovian model versions are

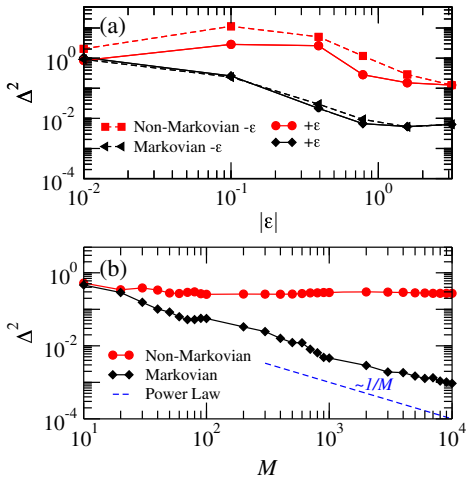

FIG. 6. Random motion in an inclined periodic potential—degree of violation for different parameters. RSD Δ^2 for Markovian (black) and non-Markovian (red) cases versus strength of the external perturbation ε for $M = 10^3$ trials (a) and versus trial number M for $\varepsilon = \pi/2$ (b). With growing number of trials M, the error for the non-Markovian case saturates, while it drops like $1/M$ for the Markovian system (b). We use Eq. (22) with $T_c = 50$.

similarly high. However, with increasing ε the RSD for the Markov process decreases to small values whereas the non-Markov model always displays values significantly different from zero. Interestingly, there is an optimal perturbation amplitude (close to our standard value $\varepsilon = \pi/2$) at which the RSD is minimal. If we increase the number of trials [Fig. 6(b)], the RSD decays like $1/M$ in the Markovian case but saturates at a nonvanishing value for the system with colored noise.

IV. RANDOM MOTION UNDER A LINEAR FORCE—A TRACTABLE EXAMPLE

Why can the NL FDR be violated for the non-Markovian case with colored noise? To better understand the underlying physics governing our NL-FDR-based test, we now pick a simple parabolic potential, the origin of which is shifted by ε until $t = T/2$:

$$V(x,t;\varepsilon) = k[x - \varepsilon\Theta(T/2 - t)]^2/2. \tag{24}$$

Equation (17) now turns into a linear equation:

$$\dot{x} = -k[x(t) - \varepsilon\Theta(T/2 - t)] + s(t). \tag{25}$$

For the unperturbed Markovian case [$\varepsilon = 0$, $s(t)$ being white Gaussian noise] this corresponds to an Ornstein-Uhlenbeck process and may, for instance, represent an overdamped particle in a harmonic trap in equilibrium [1]. For the non-Markovian case we choose $s(t)$ again to be the Ornstein-Uhlenbeck noise $\eta(t)$ generated by Eq. (18); in this case, the full system of two linear stochastic differential equations constitutes a two-dimensional Markov process whereas the variable $x(t)$ on its own must be regarded as a non-Markovian process. The system with colored noise is outside thermodynamic equilibrium because in the latter case correlations in fluctuations imply memory friction that is not present in our model.

The great advantage of this model is that all the quantities entering the NL FDR can be calculated analytically in both Markovian and non-Markovian cases, which in particular explains why in the non-Markovian version of the model a violation of the NL FDR can be expected.

First of all, because the dynamics is linear, we obtain the dynamics of the time-dependent mean value $\langle x(t)\rangle$:

$$\frac{d}{dt}\langle x\rangle = -k[\langle x(t)\rangle - \varepsilon\Theta(T/2 - t)]; \tag{26}$$

the noise term (white or colored) will drop out in the ensemble average. The solution is a simple exponential:

$$\langle x(t)\rangle = \varepsilon\begin{cases} 1 & t < T/2 \\ \exp\left[-k(t - T/2)\right] & t \geq T/2. \end{cases} \tag{27}$$

Any other time-dependent mean value will depend on t only via this mean value because we can eliminate the perturbation from the dynamics entirely when choosing a new variable $y(t) = x(t) - \langle x(t)\rangle$, for which we find

$$\dot{y} = -ky(t) + s(t). \tag{28}$$

As long as the driving noise $s(t)$ is Gaussian (no matter whether correlated or uncorrelated in time), we find that the new variable also obeys Gaussian statistics, $P_y(y) \propto \exp[-y^2/(2\sigma_x^2)]$ and thus, going back to the original variable, we have

$$P(x,t) = \exp\left[-\frac{[x - \langle x(t)\rangle]^2}{2\sigma_x^2}\right] \Big/ \sqrt{2\pi\sigma_x^2}. \tag{29}$$

The variances for the two cases can be calculated with standard methods [1,2]; for the Markovian case, it is

$$\sigma_x^2 = D/k, \tag{30}$$

whereas in the non-Markovian case, one finds

$$\sigma_x^2 = \frac{\tau_c\sigma^2}{k(1 + \tau_c k)}. \tag{31}$$

From Eq. (29), we obtain very quickly the two steady-state distributions [using $\langle x(t)\rangle$ from Eq. (27) with $t < T/2$ and $t \to \infty$ for $P_\varepsilon(x)$ and $P_0(x)$, respectively]:

$$P_\varepsilon(x) = \frac{\exp[-\frac{(x-\varepsilon)^2}{2\sigma_x^2}]}{\sqrt{2\pi\sigma_x^2}}, \qquad P_0(x) = \frac{\exp[-\frac{x^2}{2\sigma_x^2}]}{\sqrt{2\pi\sigma_x^2}}. \tag{32}$$

The two densities give us the conjugated variable:

$$z(x) = \frac{P_\varepsilon(x)}{P_0(x)} - 1 = e^{-\varepsilon^2/(2\sigma_x^2)}\exp\left[\frac{\varepsilon x}{\sigma_x^2}\right] - 1. \tag{33}$$

The conjugated variable for both Markovian and non-Markovian versions of our model is thus a simple exponential function. The Gaussian distributions and the exponential function for the conjugated variable are also found following our protocol [Figs. 7(a) and 8(a)].

In order to calculate the time-dependent mean value $\langle z[x(t)]\rangle$ in response to the perturbation arrest, we can now use the one-time probability density Eq. (29):

$$\begin{aligned}\langle z[x(t)]\rangle &= \int_{-\infty}^{\infty} dx z(x)P(x,t) \\ &= \int_{-\infty}^{\infty} dx \frac{\exp[-\frac{x^2 - 2x\langle x\rangle + \langle x\rangle^2 - 2\varepsilon x + \varepsilon^2}{2\sigma_x^2}]}{\sqrt{2\pi\sigma_x^2}} - 1 \\ &= e^{\varepsilon\langle x(t)\rangle/\sigma_x^2} - 1.\end{aligned} \tag{34}$$

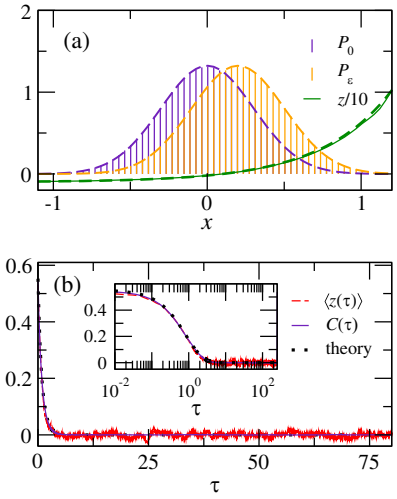

FIG. 7. Random motion with linear force—Markovian case. Equation (25) is simulated with white Gaussian noise. Measured stationary probabilities (histograms) and the conjugated variable $z(x)$ (thin solid line in green) compared to theory (dashed lines) Eqs. (32) and (33) (a). NL FDR is confirmed, as correlation function and time-dependent mean value of $z(t)$ closely agree and also match the analytical results Eqs. (35) and (41) (b). Parameters are $M = 10^4$, $T = 1000$, $\Delta t = 0.01$, $k = 1$, $\varepsilon = 0.2$, $D = 1/11$.

In particular, for $t > T/2$ we obtain

$$\langle z[x(T/2+\tau)]\rangle = \exp\left[\frac{\varepsilon^2}{\sigma_x^2}e^{-k\tau}\right] - 1. \tag{35}$$

From this expression we see that the time-dependent mean value does not depend on the temporal correlations of the noise (once we make sure by our parameter choice that both systems have the same variance σ_x^2 for the x variable). We cannot expect the same for the stationary correlations of $x(t)$—if the driving noise is very slow, for instance, we may expect that $\langle z(t)z(t+\tau)\rangle$ is affected by this and will reflect in some way the slow timescale. Hence, from the independence of the mean value of the correlation time of the noise, we may already suspect that the NL FDR has to be violated for a slow noise $\eta(t)$.

In order to calculate the correlation function for $z[x(t)]$ in the unperturbed case, we first note that the correlation function $C_{xx}(\tau)$ can be easily calculated for both Markovian and non-Markovian cases, e.g., by the Rice method for the power spectrum (Fourier transformation of the Langevin equation, multiplication with the complex conjugated equation, averaging) and a back transformation to the time domain to obtain the correlation function. This gives in the Markovian case:

$$C_{xx}(\tau) = \frac{k}{D}e^{-k|\tau|} = \sigma_x^2 e^{-k|\tau|}. \tag{36}$$

In the non-Markovian (colored noise) case we obtain

$$C_{xx}(\tau) = \frac{k}{\sigma^2\tau_c}\frac{1+\tau_c k}{1-\tau_c k}(e^{-k|\tau|} - \tau_c k e^{-|\tau|/\tau_c}) \tag{37}$$

$$= \frac{\sigma_x^2}{1-\tau_c k}(e^{-k|\tau|} - \tau_c k e^{-|\tau|/\tau_c}). \tag{38}$$

To calculate the correlation function of $z[x(t)]$, we can use that the correlation function of the new variable

$$u = he^{ax(t)} \tag{39}$$

is related to that of $x(t)$ by [see Ref. [26], Eq. (8.103)]

$$C_{uu}(t) = h^2 e^{a^2\sigma_x^2}(e^{a^2 C_{xx}(t)} - 1). \tag{40}$$

Our variable $z(x)$ according to Eq. (33) also involves an offset (we subtract 1), which does not change this result. In the Markovian case we obtain

$$C_{zz}(\tau) = \exp\left[\frac{\varepsilon^2}{\sigma_x^2}e^{-k|\tau|}\right] - 1, \tag{41}$$

which exactly agrees with the time-dependent mean value in Eq. (35). Hence, in the Markovian case, our explicit calculation of the mean value and the stationary correlation function confirms the NL FDR Eq. (8), as can be expected. For completeness, we show in Fig. 7(b) the agreement of the two statistics also by means of numerical simulation results obtained by following our protocol; they obviously agree well with each other as well as with the calculated theoretical results [Eq. (35) or (41)].

In contrast, in the non-Markovian case, Eq. (40) yields

$$C_{zz}(\tau) = \exp\left[\frac{\varepsilon^2}{\sigma_x^2}\frac{e^{-k|\tau|} - \tau_c k e^{-|\tau|/\tau_c}}{1-\tau_c k}\right] - 1, \tag{42}$$

which involves *two* exponential functions in the exponent and hence differs in its functional form qualitatively from the time-dependent mean value in Eq. (35). Only in the white noise limit, $\tau_c \to 0$ (while keeping the intensity $\sigma^2\tau_c = D$ constant), we can achieve agreement between mean value and correlation function—this is, of course, again the Markovian limit case, for which we have confirmed Eq. (8) already. For a nonvanishing value of τ_c, our result demonstrates analytically that the non-Markovian system violates the NL FDR Eq. (8). We also illustrate the violation by comparing time-dependent mean value and correlation function obtained from numerical simulations [cf. Fig. 8(b)]. Because in the example the correlation time of the colored noise was chosen rather long ($\tau_c = 100$), there is a pronounced mismatch between mean value and correlation function; as we can well understand from our analysis, the mean value quickly decays to zero (it is only determined by the timescale of the x dynamics which is set by k), whereas the correlation function has a

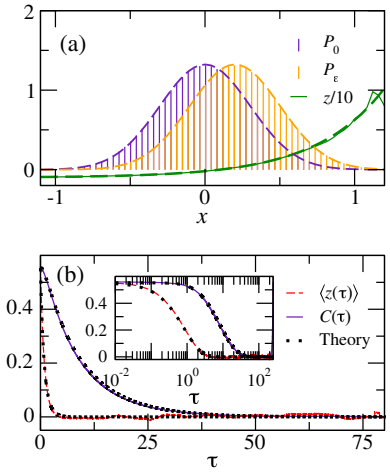

FIG. 8. Random motion with linear force—non-Markovian case. Equation (25) is simulated with colored noise $s(t) = \eta(t)$ obeying Eq. (18). Measured stationary probabilities (histograms) and conjugated variable $z(x)$ (green solid line) compared to theory (dashed lines) Eqs. (32) and (33) (a). Mean value and correlation function differ as revealed by the simulation results (lines) and the theoretical expressions (points), Eqs. (35) and (42) (b). Parameters are $M = 10^4$, $T = 1000$, $\Delta t = 0.01$, $F = 1$, $\varepsilon = 0.2, \sigma^2 = 0.1$, $\tau = 10$.

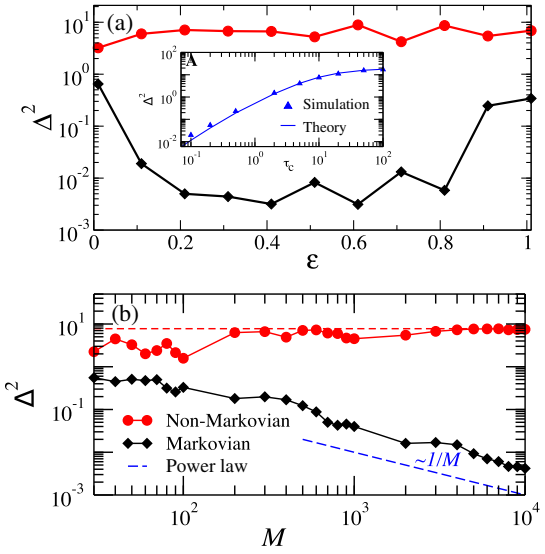

FIG. 9. Random motion with linear force—quantifying the NL FDR violation. RSD Eq. (22) for an integration window of $T_c = 10$ and $M = 10^4$ as a function of perturbation strength ε for the Markovian (black) and the non-Markovian setup (red); inset shows Δ^2 as a function of the correlation time τ_c of the colored noise [theory is obtained using Eqs. (35) and (42) in Eq. (22)]. For $\tau_c = 10$, RSD of the non-Markovian system (red) versus number of trials M (theory value for $M \to \infty$ indicated by dashed line); RSD of the Markov version (black) decays like a power law $1/M$.

part that decays much slower because it is set by the correlation time τ_c.

We quantify the violation of the NL FDR by the RSD Δ^2 in Fig. 9 as a function of different parameters. The non-Markovian case (red) reveals itself by high RSD, whereas in the Markovian case (black) the RSD is generally rather small. If we increase the amplitude of the perturbation ε [Fig. 9(a)], we first gain from leaving the linear-response regime—here, differences between the RSD of non-Markovian and Markovian cases become more pronounced. However, in the Markovian case, after having passed through a broad minimum, Δ^2 increases again—if the amplitude becomes too large ($\varepsilon \gg \sigma_x \approx 0.3$) there is only little overlap between the two probability densities, making the determination of $z(x)$ and its statistics unreliable.

For the non-Markovian case, the RSD grows with the correlation time τ_c of the colored noise increases [inset in Fig. 9(a)]. If we fix the correlation time and plot the RSD as a function of the trial number M, the RSD of the Markovian system decays like $1/M$, whereas that of the Markovian system saturates.

We finally mention that for Eq. (25) studied here, we can easily calculate an exact (and different) FDR in terms of the original variable $x(t)$, which is for this specific linear system not limited to weak perturbations.

V. TESTING THE NL FDR EXPERIMENTALLY FAR FROM THERMAL EQUILIBRIUM

In this section we describe an experiment aimed at testing the applicability and the benefits of the NL FDR.

A. Experimental setup

We realize experimentally a stochastic nonequilibrium system of a fluctuating particle in a harmonic potential (see Fig. 10) as described below. An ensemble of bristlebots and a styrofoam ball are placed inside a parabolic plastic bowl, acting as a gravitational harmonic well. Collisions between the bots keep them in a chaotic state, in which they act as an active bath on the styrofoam ball, our tracer particle (see Movie 1 in Supplemental Material [27]). The locomotive motion of bristlebots as well as their individual dynamics in a gravitational harmonic potential was studied before [28]. Here we use a system with either 10 or 4 bristlebots with an effective area fraction of 8% and 5%, respectively, and focus on the statistics of the random motion of the tracer particle.

In order to test the NL FDR in the experiment, we use a fan (Yate Loon electronics 12 V 0.30 A cooling fan) and shutter system to perturb the trajectory of the tracer particle. The air stream emanating from the fan exerts a uniform external force on the styrofoam ball but barely affects the bristlebots. To ensure a sudden deactivation (activation) of the perturbing force, we add a shutter to cut off the transient behavior of the fan and achieve thus an abrupt perturbation arrest. The magnitude of the applied perturbation is controlled by the operating voltage of the fan. Summarizing, the main forces acting on the tracer ball are due to the gravitational potential, the air stream from the fan, and the random collisions with the bristlebots.

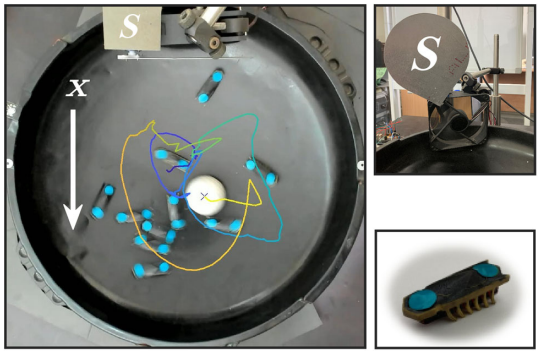

FIG. 10. Experimental setup. A styrofoam ball (diameter ∼4 cm) is trapped in a gravitational harmonic potential, a plastic bowl (diameter 38 cm, depth 5 cm), and subjected to collisions with self-propelled bristlebots (inset: standard bot, 4×1 cm). The ball is repeatedly perturbed with a uniform air stream created by an external fan to test the NL FDR. To enforce an abrupt onset and release of the perturbation, a mechanical shutter is used (denoted by "S"). A typical trajectory of the styrofoam ball perturbed by ten bristlebots is plotted (time color coded); see also Movie 1 in Supplemental Material [27]. The response to the air stream arrest is measured along the x axis (white arrow).

We image a top view of the experiments using a logitech-BRIO 4k camera at a frame rate of 30 fps. Because of the finite energy storage of the bristlebot battery, the duration of the experiments is limited to 30 min. We extract the trajectories of the styrofoam ball using standard MATLAB algorithms. Finally, we project the trajectory of the tracer onto the axis of the direction of the air stream. We choose a macroscopic experimental system for several reasons. First, the system is clearly out of equilibrium, being composed of active matter (the bristlebots). The steady state relies on constant injection of energy and its dissipation to the environment (friction within the bowl and with the surrounding air). Second, the system can be easily monitored, controlled, and perturbed mechanically, and there are obviously no significant thermal contributions. Finally, the dynamics of a tracer ball interacting with the bots in the bowl is similar to that of a colloidal particle in a harmonic potential, discussed in Sec. IV: In both cases the tracer particle is bound by a confining potential and experiences random collisions.

B. Quantifying the advantage of the NL FDR

We start by measuring the statistics needed for the NL FDR Eq. (8) and the linear version Eq. (15) in a system of 10 bristlebots and a fan operating at 12 V. Specifically, we apply an external force with the fan on the styrofoam ball in the following sequence: every 2 min the fan is turned on for a minute and abruptly turned off for the following minute, which could be done 15 times in the 30 min of one recording. This sequence of perturbations was repeated throughout each of the 25 recordings resulting in a total of 375 experimental trials. Following the analysis protocol of Fig. 3, we first obtain the time-dependent tracer position along the perturbation direction. In Fig. 11(a) we show the time-dependent mean value of these positions, which illustrates that the two steady states in phases II and IV and the transition between them are well captured within our time window.

For further analysis, we extract the steady-state position probability densities, with and without a perturbing force, and the conjugated variable calculated from them via Eq. (5) [all functions are shown in Fig. 11(b)]. The two quantities of the NL FDR can now be evaluated. The response to the perturbation arrest in terms of the mean conjugated variable is obtained from section III (red) of the time window; the correlations of the stationary fluctuations in the absence of the perturbation were calculated from section IV (violet). These two quantities are plotted in Fig. 11(c) (their standard errors are indicated by the dashed lines). When comparing the response and the correlation function, we focus on the initial part, up to a time $T_c = 1$ s, indicated by a vertical line in Fig. 11(c) [time at which $\langle z \rangle$ reach the standard error of the mean value estimate in the steady state].

As before, we quantify how well the NL FDR is satisfied (or not) by the RSD, Eq. (22). Figure 11(d) displays the RSD versus number of trials M. This analysis is highly

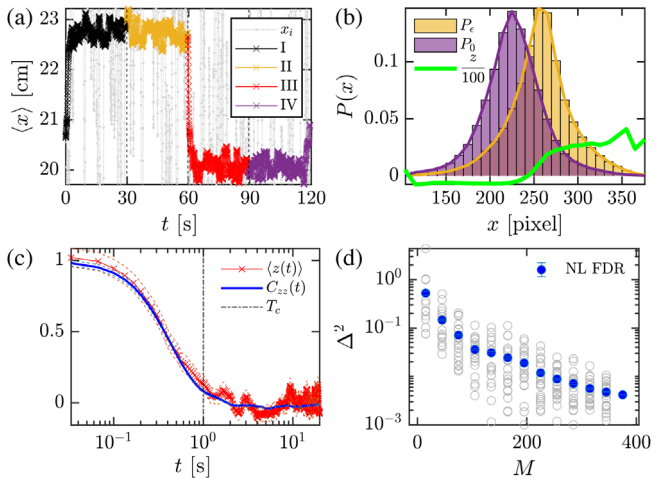

FIG. 11. Experimental test of the NL FDR with bristlebots. Ensemble mean of position $\langle x_i(t) \rangle$ (bold line, color coded according to phase) and a single trajectory $x_i(t)$ (gray line); averages were calculated over $M = 375$ trials (a). Probability densities of the two steady states of the periods II (P_e, yellow) and IV (P_0, violet) overlayed by the conjugated variable (green line); histograms are normalized and linearly interpolated (b). Transient response $\langle z(t) \rangle$, and the autocorrelation $C_{zz}(t)$, from periods III and IV, respectively, as functions of time (dashed lines indicate standard errors); up to time T_c (dash-dotted line), both curves agree well (c). Deviations from the NL FDR are quantified by the RSD versus trial number (d), integrated up to time T_c [gray points are subsets of trials (see text); blue points are average of these separate computations]. We use ten regular bristlebots with a fan operating at 12 V, for driving cycles of $T = 2$ min.

sensitive to the choice of subset of trials that we select. We therefore repeat this computation for different subsets of trials [gray data points in Fig. 11(d)]. The colored data points are the average of these separate calculations. Clearly, the RSD drops toward zero as the number of trials increases, indicating that the NL FDR Eq. (8) holds in these conditions. Hence, our results are consistent with a Markovian dynamics of the tracer particle.

At first glance, the interaction of a few bristlebots with the styrofoam ball cannot be expected to yield strictly Markovian dynamics for the styrofoam ball. Nevertheless, our results suggest that under the inspected conditions the effective dynamics of the light ball could not be proven to be pronouncedly non-Markovian. This, of course, is not a proof of Markovianity in itself but supports at least this simplifying assumption. We interpret this result as follows. Since the ball is light (possesses little inertia) and collisions with the chaotically moving bristlebots are frequent, we may expect an approximate Markovian dynamics, i.e., a loss of memory, at timescales larger then the typical time between collisions, and thus the NL FDR should hold.

We also remark that although the true motion of the styrofoam ball within the bowl is two dimensional, there seems to be little effect of the motion in the direction perpendicular to the air stream. This is similar to an extension of our model of a harmonically trapped particle Eq. (25) to two spatial dimensions by an addition of an independent second equation,

$$\dot{x}_2 = -kx_2 + \sqrt{2D}\xi_2(t), \tag{43}$$

with $\xi_2(t)$ being an independent white Gaussian noise and no perturbation included. Then the original dynamics $x(t)$ would still be Markovian and our test would also confirm the NL FDR as before. This argument does not hold true in a nonlinear two-dimensional system, in which both variables affect each other; see Ref. [5] for an example.

To emphasize the advantages of the nonlinear relation as a test for Markovianity for nonequilibrium systems, we examin both the linear and the nonlinear relations under weak (fan at 9 V) and strong (fan at 12 V) perturbations, for an otherwise identical setup. The results for these two conditions are displayed in Figs. 12(a) and 12(b). The insets test the linear relation, Eq. (15), obtained by following the same protocol for the linear conjugated variable, Eq. (14) (see also Ref. [5]). We can see a pronounced violation of the linear relation, Eq. (15) [with the conjugated variable defined by Eq. (14)] for the strong perturbation, Fig. 12(b), while both linear relation and NL FDR are obeyed for the weak perturbation, Fig. 12(a). This result confirms that the NL FDR of Eq. (8) is fulfilled even in the presence of a strong perturbation, where the linear version is violated. Moreover, in the nonlinear-response regime, the NL FDR requires significantly fewer data to capture the response. Specifically for the presented data, the same small RSD

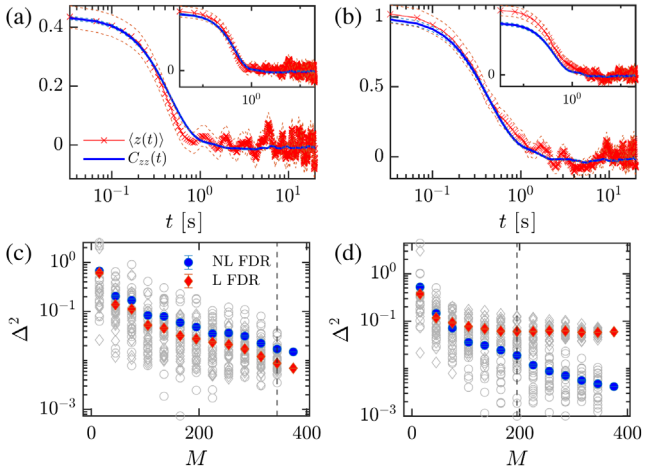

FIG. 12. Linear and nonlinear FDR under weak and strong perturbation [9 V fan voltage (a),(c) and 12 V fan voltage (b),(d)]. Panels (a) and (b) display mean responses and correlation functions for the NL FDR (main panels) and the linearized version, Eq. (15) (insets), all for $M = 375$ trials. Panels (c) and (d) show the RSD versus number of trials for the weak (c) and strong perturbation (d) for the linear (orange diamonds) and nonlinear relations (blue circles). The vertical dashed lines correspond to the minimal M above which $\Delta^2 < 0.02$. Other parameters as in Fig. 11.

value of $\Delta^2 = 0.02$ can be reached in the strong-fan configuration with only 195 trials [see vertical dashed line in Fig. 12(c)], whereas 345 trials are required to reach the same degree of quantitative agreement for the linear version [cf. vertical dashed line Fig. 12(d)]. In conclusion, the nonlinear FDR requires less experimentation time and is thus better suited for situations in which only a limited number of trials is feasible.

C. Violation of the NL FDR for a slowly changing active bath

To provoke a violation of the NL FDR we construct a non-Markovian system by using a two-sided model of bristlebots [Fig. 13(a)]. This model of bristlebots can move on either side, since it has bristles on both top and bottom [see Fig. 13(a) herein and Movie 2 in Supplemental Material [27]). We refer to these two types of motion as *up* (↑) and *down* (↓) states with respect to the side on which the bot moves. Interestingly, the bristlebots can flip between states upon collisions and the motion in the up state is slower [cf. Fig. 13(b)] and less stable [cf. Fig. 13(c), where $\tau_{\uparrow\downarrow} \ll \tau_{\downarrow\downarrow}$]. We refer to the state of the bath as a mixed (uniform) state if at least one (none) bath particle is in the up state. The average lifetimes of the two states of the bath are $\langle\tau_{\uparrow\downarrow}\rangle = 0.5$ s and $\langle\tau_{\downarrow\downarrow}\rangle = 2.3$ s. Since $\langle\tau_{\uparrow\downarrow}\rangle, \langle\tau_{\downarrow\downarrow}\rangle$ are of the order of the typical relaxation time of the system, we expect non-Markovianity to arise. Our approach to provoke non-Markovianity is reminiscent of

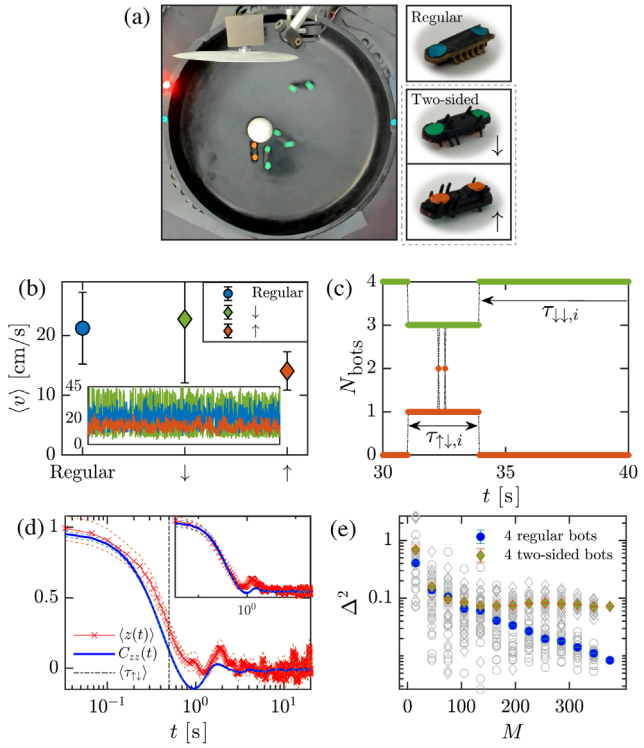

FIG. 13. Experimental system with non-Markovian features. Top view snapshot (a) of a mixed ($\uparrow\downarrow$) state with three particles in the $\downarrow$ state (green) and one in the $\uparrow$ state (orange). The two different types of bristlebots are shown on the right: regular (top) and the two configurations of the two-sided bristlebot (bottom). The average individual speeds (b) of the $\downarrow$ state (green diamond), the $\uparrow$ state (orange diamond), and the regular bristlebot (blue circle). The inset displays typical sequences of instantaneous speed $v(t)$ in cm/s for the regular (blue) and two-sided (green $\downarrow$, orange $\uparrow$) bots over 30 s. Number of bots in each state with one bot flipping back and forth (c). Violation of the NL FDR, Eq. (8), at $\tau \approx 1$ s, obtained for an average of $M = 375$ trials and a strong perturbation, implies non-Markovian dynamics (d). For comparison, an equivalent experiment for four regular bristlebots, which does not display a significant violation of the NL FDR below T_c (inset). Comparison of the RSD (e) with $T_c = 1$ s for the two types of experiments in (d). Unlike the system of regular bristlebots, the RSD of the two-sided bristlebot system does not decay to zero, indicating a systematic violation of the NL FDR.

the recent study [29] in which an optically trapped colloidal particle was driven by a telegraph noise.

To test for non-Markovianity, we conduct a fluctuation-dissipation experiment with four two-sided bristlebots using the same experimental procedure as in Sec. V B [see Fig. 13(d)]. A violation of the relation becomes apparent for times around the average lifetime of the mixed state $\langle \tau_{\uparrow\downarrow} \rangle$ (horizontal dot-dashed line), implying non-Markovian dynamics. For comparison, the inset of Fig. 13(d) shows the NL FDR for the four regular bristlebot system. In this case, the NL FDR holds, consistent with Markovian dynamics of the tracer particle.

The non-Markovian version in the experiment is more sophisticated than in the theoretical models and involves the "heat bath" itself. Having bristlebots with two different states of speed between which occasionally stochastic transitions occur introduces a slow timescale in the system, that (comparable to the colored noise in the theoretical models) modifies the temporal correlations of the conjugated variable but not so much its time-dependent mean value after the switch-off. For this variant of the experiment a significant deviation from the NL FDR could be observed (with just a few hundred trials necessary).

VI. DISCUSSION AND OUTLOOK

Fluctuation-response relations have been previously studied beyond the linear-response regime [14,19,30,31]. However, two important aspects of these relations are still poorly understood so far: (i) how Markovianity is a needed precondition and how the nonlinear FDR is violated for non-Markovian systems and (ii) how the number of experimental or simulation trials can be substantially reduced by exploiting the nonlinear response. In this paper we investigate these aspects for a novel fluctuation-dissipation relation for a nonweak perturbation of a Markovian system, the NL FDR. We develop a simple protocol tailored to probe the relation in simulations of stochastic models or in experiments. We test it for two paradigmatic models of statistical physics: the random motion in a biased washboard potential and the harmonically bound particle with noise. Furthermore, we explore the NL FDR for an experimental toy model: a styrofoam ball embedded in an active bath of bristlebots placed in a parabolically shaped bowl.

We succeed in our goal to utilize stronger perturbations to decrease the amount of data needed for a test of Markovianity in comparison with the linear-response version of the relation [10–14]. Differences between Markovian and non-Markovian cases in Figs. 6(b) and 9(b) emerge already for a few tens of trials; it is unlikely that Markovianity can be tested with statistical significance with much fewer data. A significant improvement of the test's applicability is also shown in our experiments, in which the amount of data needed is reduced by roughly one-half compared to linear-response conditions. The comparison of the efficiency of our method to other tests of Markovianity (see, for instance, Refs. [6,7,9]) is an open problem for future studies.

We emphasize that the main element of our scheme for testing the NL FDR, a perturbation in the form of a step stimulus, is already part of many experimental standard protocols for nonequilibrium systems [15–18]. Our method could be used to reinspect systems for which linear-response-based fluctuation-dissipation theorems have been tested in the past [4,32,33].

An additional outcome of our analysis is the existence of an optimal amplitude of perturbation. From Figs. 1(b) and 3(b) it can be seen that the conjugated variable is most

informative when the overlap between $P_0(x)$ and $P_\varepsilon(x)$ is not too large or too small. An optimal perturbation amplitude and hence overlap is seen in Fig. 6(a) for the motion in a biased periodic potential, where the RSD in the Markovian case attains its minimum at $\varepsilon = \pi/2$. Even more pronounced is the minimal RSD for the harmonically bound particle [Fig. 9(a)]. How the perturbation amplitude can be optimized in different systems and for different kinds of perturbations remains an exciting problem for future investigations.

Notably, the analytically tractable case of the harmonically bound particle with colored noise permits us to trace one cause for the violation of the NL FDR for a non-Markovian dynamics. While the mean value of the conjugated variable is not affected at all by the correlations of the driving fluctuations, the correlations of $z(t)$ are shaped by the noise color. We thus recognize the reason why these two kinds of statistics disagree in general in the non-Markovian setting. Qualitatively, the same holds true for the random motion in the biased periodic potential, for which the time-dependent mean value $\langle z(t)\rangle$ decays rather quickly after the perturbation is switched off, whereas the correlations of $z(t)$ in the unperturbed state display a slow component due to the colored noise.

Having introduced the idea of using stronger perturbation for more practical test for Markovianity, it is natural to ask whether we can further minimize the required statistics. First, the procedure itself can be optimized. Statistics can be doubled by using both switch-off and switch-on perturbations (provided they are abrupt). In addition, the phase durations of the protocol can be chosen as different according to need. Second, the general form of the NL FDR Eq. (6) relates the time-dependent mean value of an arbitrary observable $f[x(t)]$ with the stationary cross-correlation function of the very same observable $f[x(t')]$ and the conjugated variable $z[x(t)]$. Are there choices of the function $f(x)$ that lead to particularly significant tests of Markovianity? Finally, different perturbations from those discussed here may lead to new tests of Markovianity with different conjugated variables.

The set of ideas developed in this paper can be extended to other stochastic nonequilibrium systems and to multidimensional systems. In conclusion, our work lays the foundation for a simple model-free experimental classification of a diverse nonequilibrium system in terms of Markovianity.

ACKNOWLEDGMENTS

D. B. and Y. R. acknowledge support from the European Research Council (ERC) under the European Union's Horizon 2020 research innovation programme (Grant agreement No. 101002329). This research was funded by the Deutsche Forschungsgemeinschaft (DFG, German Research Foundation) as part of the SPP 2205—LI 1046/1 (B. L.).

[1] H. Risken, *The Fokker-Planck Equation* (Springer, Berlin, 1984).
[2] C. W. Gardiner, *Handbook of Stochastic Methods* (Springer-Verlag, Berlin, 1985).
[3] N. G. van Kampen, *Stochastic Processes in Physics and Chemistry* (North-Holland, Amsterdam, 1992).
[4] L. Dinis, P. Martin, J. Barral, J. Prost, and J. F. Joanny, *Fluctuation-Response Theorem for the Active Noisy Oscillator of the Hair-Cell Bundle*, Phys. Rev. Lett. **109**, 160602 (2012).
[5] L. Willareth, I. M. Sokolov, Y. Roichman, and B. Lindner, *Generalized Fluctuation-Dissipation Theorem as a Test of the Markovianity of a System*, Europhys. Lett. **118**, 20001 (2017).
[6] A. M. Berezhkovskii and D. E. Makarov, *Single-Molecule Test for Markovianity of the Dynamics along a Reaction Coordinate*, J. Phys. Chem. Lett. **9**, 2190 (2018).
[7] A. M. Berezhkovskii and D. E. Makarov, *On the Forward/Backward Symmetry of Transition Path Time Distributions in Nonequilibrium Systems*, J. Chem. Phys. **151**, 065102 (2019).
[8] R. Satija, A. M. Berezhkovskii, and D. E. Makarov, *Broad Distributions of Transition-Path Times Are Fingerprints of Multidimensionality of the Underlying Free Energy Landscapes*, Proc. Natl. Acad. Sci. U.S.A. **117**, 27116 (2020).
[9] A. Lapolla and A. Godec, *Toolbox for Quantifying Memory in Dynamics along Reaction Coordinates*, Phys. Rev. Res. **3**, L022018 (2021).
[10] G. S. Agarwal, *Fluctuation-Dissipation Theorems for Systems in Non-Thermal Equilibrium and Applications*, Z. Phys. **252**, 25 (1972).
[11] P. Hänggi and H. Thomas, *Stochastic Processes: Time Evolution, Symmetries and Linear Response*, Phys. Rep. **88**, 207 (1982).
[12] J. Prost, J.-F. Joanny, and J. M. R. Parrondo, *Generalized Fluctuation-Dissipation Theorem for Steady-State Systems*, Phys. Rev. Lett. **103**, 090601 (2009).
[13] J. R. Gomez-Solano, A. Petrosyan, S. Ciliberto, R. Chetrite, and K. Gawedzki, *Experimental Verification of a Modified Fluctuation-Dissipation Relation for a Micron-Sized Particle in a Nonequilibrium Steady State*, Phys. Rev. Lett. **103**, 040601 (2009).
[14] C. Maes, *Response Theory: A Trajectory-Based Approach*, Front. Phys. **8**, 229 (2020).
[15] A. E. Ekpenyong, G. Whyte, K. Chalut, S. Pagliara, F. Lautenschläger, C. Fiddler, S. Paschke, U. F. Keyser, E. R. Chilvers, and J. Guck, *Viscoelastic Properties of Differentiating Blood Cells Are Fate- and Function-Dependent*, PLoS One **7**, 1 (2012).
[16] A. Hudspeth, Y. Choe, A. D. Mehta, and P. Martin, *Putting Ion Channels to Work: Mechanoelectrical Transduction, Adaptation, and Amplification by Hair Cells*, Proc. Natl. Acad. Sci. U.S.A. **97**, 11765 (2000).
[17] G. Nagel, M. Brauner, J. F. Liewald, N. Adeishvili, E. Bamberg, and A. Gottschalk, *Light Activation of Channelrhodopsin-2 in Excitable Cells of Caenorhabditis elegans Triggers Rapid Behavioral Responses*, Curr. Biol. **15**, 2279 (2005).
[18] K. Thurley, S. C. Tovey, G. Moenke, V. L. Prince, A. Meena, A. P. Thomas, A. Skupin, C. W. Taylor, and M. Falcke,

Reliable Encoding of Stimulus Intensities within Random Sequences of Intracellular Ca^{2+} *Spikes*, Sci. Signal. (Online) **7**, ra59 (2014).

[19] G. Boffetta, G. Lacorata, S. Musacchio, and A. Vulpiani, *Relaxation of Finite Perturbations: Beyond the Fluctuation-Response Relation*, Chaos **13**, 806 (2003).

[20] U. M. B. Marconi, A. Puglisi, L. Rondoni, and A. Vulpiani, *Fluctuation-Dissipation: Response Theory in Statistical Physics*, Phys. Rep. **461**, 111 (2008).

[21] J. Mehl, V. Blickle, U. Seifert, and C. Bechinger, *Experimental Accessibility of Generalized Fluctuation-Dissipation Relations for Nonequilibrium Steady States*, Phys. Rev. E **82**, 032401 (2010).

[22] C. Yolcu, A. Berut, G. Falasco, A. Petrosyan, S. Ciliberto, and M. Baiesi, *A General Fluctuation Response Relation for Noise Variations and Its Application to Driven Hydrodynamic Experiments*, J. Stat. Phys. **167**, 29 (2017).

[23] S. Ciliberto, R. Gomez-Solano, and A. Petrosyan, *Fluctuations, Linear Response, and Currents in Out-of-Equilibrium Systems*, Annu. Rev. Condens. Matter Phys. **4**, 235 (2013).

[24] P. Reimann, C. Van den Broeck, H. Linke, P. Hänggi, J. M. Rubi, and A. Pérez-Madrid, *Giant Acceleration of Free Diffusion by Use of Tilted Periodic Potentials*, Phys. Rev. Lett. **87**, 010602 (2001).

[25] P. Reimann, *Brownian Motors: Noisy Transport Far from Equilibrium*, Phys. Rep. **361**, 57 (2002).

[26] R. L. Stratonovich, *Topics in the Theory of Random Noise* (Gordon and Breach, New York, 1967).

[27] See Supplemental Material at http://link.aps.org/supplemental/10.1103/PhysRevX.13.021034 for Supplemental Movie [1]–The System: Different number of (standard) bristlebot ensembles are shown as they collide in a parabolic dish, resulting in their stochastic motion. The tracer (Styrofoam) ball is trapped in the gravitational harmonic potential, and fluctuates due to collisions with the bots. Once the fan is switched on and the shutter opens, the mean position of the tracer is shifted from the trap center, and the two perturbed and unperturbed steady states are measured and Supplemental Movie [2]–Non-Markovian Setup: The two distinct states of the two-sided bot model are shown, as described in the text. The "up" state is characterized as the stable state, with a higher velocity. The ensemble of bots is in a "uniform" state once all the bots are in the "up" state. A "mixed" state is reached once at least one bot is in the "down" state.

[28] O. Dauchot and V. Démery, *Dynamics of a Self-Propelled Particle in a Harmonic Trap*, Phys. Rev. Lett. **122**, 068002 (2019).

[29] J. Gladrow, M. Ribezzi-Crivellari, F. Ritort, and U. F. Keyser, *Experimental Evidence of Symmetry Breaking of Transition-Path Times*, Nat. Commun. **10**, 55 (2019).

[30] K. I. Golden, G. Kalman, and M. B. Silevitch, *Nonlinear Fluctuation-Dissipation Theorem*, J. Stat. Phys. **6**, 87 (1972).

[31] V. Lucarini and M. Colangeli, *Beyond the Linear Fluctuation-Dissipation Theorem: The Role of Causality*, J. Stat. Mech. (2012) P05013.

[32] D. Mizuno, C. Tardin, C. F. Schmidt, and F. C. MacKintosh, *Nonequilibrium Mechanics of Active Cytoskeletal Networks*, Science **315**, 370 (2007).

[33] H. Turlier, D. A. Fedosov, B. Audoly, T. Auth, N. S. Gov, C. Sykes, J. F. Joanny, G. Gompper, and N. Betz, *Equilibrium Physics Breakdown Reveals the Active Nature of Red Blood Cell Flickering*, Nature (London) **12**, 513 (2016).